BMC Plant Biology

RESEARCH Open Access

# Predicting suitable habitats of parasitic desert species based on Biomod2 ensemble model: *Cynomorium songaricum* rupr and its host plants as an example

Lucun Yang[1*], Huamei Jia[2] and Qing Hua[3]

## Abstract

**Background** As a species of considerable medicinal, ecological, and economic significance, the protection of *C. songaricum* and its host plants is of paramount importance. Biodiversity patterns and species distribution are profoundly influenced by climate change. Understanding the adaptive mechanisms of organisms in response to these changes is essential for effective species conservation. However, there is currently limited information available on simulating habitat suitability and assessing key environmental factors associated with parasite species using niche models.

**Methods** This study utilized environmental and species distribution data to analyze the shifts in the geographic range of *C. songaricum* and its host plants under current and projected future climate scenarios using the Biomod2 platform, which integrates multiple individual models into an ensemble framework. Additionally, the study quantified the environmental variables influencing the observed distribution patterns.

**Results** The potential geographical distribution and overlapping areas of *C. songaricum* and its host plants are primarily concentrated in Asia and North America. Under all four scenarios within the two timeframes (2041–2060 and 2061–2080), the overall suitable habitat areas for *C. songaricum*, *Nitraria tangutorum* Bobr., *N. sphaerocarpa* Maxim., and *Peganum multisectum* (Maxim.) Bobrov are expected to decrease compared with current climatic conditions. Conversely, the total area of suitable habitat for *Kalidium foliatum* (Pall.) Moq., *Nitraria sibirica* Pall., and *Zygophyllum xanthoxylum* (Bunge) Maxim. is predicted to increase. All species except *K. foliatum* will experience greater reductions between 2041 and 2060 than between 2061 and 2080 under more severe climate change scenarios. There is significant ecological niche overlap among *C. songaricum*, *N. sphaerocarpa*, *N. tangutorum*, and *P. multisectum*. Key factors influencing the future distribution of *C. songaricum* include the mean ultraviolet-B light of the lowest month, altitude, and annual mean temperature.

**Conclusion** A comprehensive analysis demonstrated that the accuracy of predictions could be significantly enhanced and the distributional error for individual species could be minimized by employing the Biomod2

*Correspondence:
Lucun Yang
yanglucun@nwipb.cas.cn

Full list of author information is available at the end of the article

© The Author(s) 2025. **Open Access** This article is licensed under a Creative Commons Attribution-NonCommercial-NoDerivatives 4.0 International License, which permits any non-commercial use, sharing, distribution and reproduction in any medium or format, as long as you give appropriate credit to the original author(s) and the source, provide a link to the Creative Commons licence, and indicate if you modified the licensed material. You do not have permission under this licence to share adapted material derived from this article or parts of it. The images or other third party material in this article are included in the article's Creative Commons licence, unless indicated otherwise in a credit line to the material. If material is not included in the article's Creative Commons licence and your intended use is not permitted by statutory regulation or exceeds the permitted use, you will need to obtain permission directly from the copyright holder. To view a copy of this licence, visit http://creativecommons.org/licenses/by-nc-nd/4.0/.

ensemble model to simulate the suitable habitats of parasitic species. The findings of this study can significantly inform both the management of *C. songaricum* plantations and the conservation of *C. songaricum* and its host plants.

**Keywords** Parasitic species, Suitable habitat, Species distribution modelling, Ensemble model

## Introduction

*Cynomorium songaricum* Rupr., commonly known as the "elixir of youth," is a monotypic species within the Cynomoriaceae family [1]. This fully parasitic seed plant predominantly attaches to the roots of various families, including Zygophyllaceae, Nitrariaceae, and Chenopodiaceae, and specifically genera such as *Nitraria* L., *Peganum* L., *Kalidium* Moq., and *Sarcozygium* Bunge [2]. It is renowned for its therapeutic functions in nourishing the kidney yang, enhancing essence and blood production, and promoting intestinal lubrication and bowel movements. Research indicates that *C. songaricum* possesses significant medicinal value in cancer prevention and treatment, immune regulation, delay in aging, cardiovascular disease management, and leukopenia therapy [3–5]. In Mongolian medicine, it is also utilized for alleviating diarrhoea, improving appetite, treating intestinal heat conditions, such as gastritis and indigestion, and treating dysentery [6–7]. Recently, functional health foods derived from *C. songaricum* have garnered considerable attention and popularity; examples include *C. songaricum* oil cake, polysaccharide chewable tablets of *C. songaricum*, and *C. songaricum* wine [8]. Consequently, as a dual-purpose food-medicinal plant, the demand for *C. songaricum* has been increasing. However, this heightened demand has led to the progressive depletion of wild *C. songaricum* resources due to detrimental harvesting practices and market pressures. Additionally, owing to their distinct physiological and morphological attributes and adaptability to desert ecosystems, *C. songaricum* and its host plants constitute the predominant species in arid zones. They play a vital role in safeguarding existing natural grasslands, averting desertification, rehabilitating vegetation, and enhancing the local ecological milieu [9]. Nevertheless, with the increasing exploitation and utilization value of *C. songaricum*, excessive extraction for personal gain has caused substantial damage to host plants, adversely affecting their reproductive rates and exacerbating soil erosion. This not only undermines the ecological environment but also compromises their intrinsic functions. In conclusion, the protection of wild *C. songaricum* and its host plant resources is urgently needed to ensure sustainable ecological balance and preserve their medicinal and ecological significance.

Establishing conservation areas and conducting artificial cultivation are the two most prominent approaches for protecting *C. songaricum* and its host wild resources. One of the essential techniques in the conservation of wild resources, particularly for *C. songaricum* and its host plants, involves identifying suitable habitats based on species-specific responses to spatially distributed environmental conditions [10]. The artificial cultivation of *C. songaricum* is influenced by topographical features, soil types, and climatic factors such as temperature, humidity, and precipitation [11–12]. Additionally, wind direction is crucial, as high wind speeds can disperse seeds and seedlings over considerable distances. Moreover, biophysical characteristics, including soil deposition, hydrological responses, and drainage, play pivotal roles in determining habitat suitability for plant communities [13]. Microclimatic conditions are also regarded as critical determinants of suitable habitats. However, this task is challenging due to the overlapping resource requirements among different plant species within a community [14]. Therefore, identifying suitable habitats for *C. songaricum* and its host plants while understanding the primary factors influencing each species facilitates effective restoration and revegetation planning.

Species distribution modelling, or SDM, is a critical tool for investigating ecological concerns pertaining to species and environments in the context of global change [15–16]. SDM is extensively employed in research regarding effects of climate change on species distributions and in protected area planning [17–23]. Numerous studies have employed SDM in research on wild medicinal resources for predicting the distribution of medicinal species and identifying conservation areas [24–26]. However, many studies that estimate changes in the ranges of medicinal species in China and neighboring regions in response to climate change have primarily focused on nonparasitic medicinal plants, such as unique or endangered species [27–32]. To date, only a limited number of studies have addressed parasitic medicinal plants [33–34]. As a holoparasitic species, *C. songaricum* derives all its nutrients from its host plants, with its entire growth and developmental processes occurring within the host's root system [35–36]. Consequently, unlike nonparasitic plants, the distribution of parasitic species like *C. songaricum* is influenced not only by abiotic factors but also by host factors [33–34]. Previous studies have demonstrated that for holoparasitic plants, host factors are particularly significant, especially in species distribution modelling [33–34].

The predictive functions of algorithms (modelling techniques) that link occurrence data (dependent variables) to independent variables (environmental factors) may introduce uncertainties [37–39]. The selection of a modelling algorithm is a primary source of uncertainty

in the performance and spatial predictions of species distribution models (SDMs), as different algorithms adopt varying approaches to the interactions between species occurrence and environmental conditions. Given the multitude of available algorithms, each with distinct advantages, selecting the most suitable SDM algorithm poses a significant challenge [40–43]. Consequently, it is crucial to identify which modelling technique performs optimally; employing an inappropriate method could lead to overestimations or inaccuracies in species distribution predictions [42–45]. Currently, numerous distributed prediction models have been developed and applied. Among the most widely used niche models are maximum entropy (MaxEnt) [19], random forest (RF) [20], and generalized linear model (GLM) [21]. However, these models vary in their principles, assumptions, and algorithms, leading to differences in predictive performance. Different modelling techniques for the same species can yield divergent results [46], and specific variations often exist between species [47]. An increasing number of researchers are working on integrating multiple models to mitigate the instability caused by different principal algorithms or variations in input data [25]. Biomod2, an integrated prediction platform for species distributions developed in R, comprehensively evaluates current species distributions and integrates models with higher accuracy to predict future species distributions [48–49]. To date, the Biomod2 ensemble model has been utilized to forecast the probable geographic ranges of numerous species [50–53], but few studies have focused on predicting the potential geographical distributions of parasitic species. Therefore, studying the habitat suitability of parasitic species using the Biomod2 ensemble model is of utmost importance.

Using optimistic, intermediate, and pessimistic climate change scenarios, this study estimates changes in the potential ranges of *C. songaricum* and its hosts in China and the neighbouring countries of China for 2041–2060 and 2061–2080. These species play important roles in desert ecosystems.

This study is the first to adopt the Biomod2 integrated modeling technology to screen and optimize the ecological model, and systematically predict the potential suitable planting areas of *C. songaricum* and its host plants (such as *N. tangutorum*, *N. sphaerocarpa*, *K. foliatum*, *N.sibirica*, *Z. xanthoxylum* and *P. multisectum*) under climate change. The research objectives include: (1) Comparing the prediction accuracy of *C. songaricum* and its host plants based on the ten models provided by Biomod2 (GLM, GBM, RF, etc.); (2) Predicting the potential geographical distribution of *C. songaricum* and its host plants under the current climate conditions, and classifying the suitable areas (high, medium, and low suitable areas); (3) Determining the key environmental factors that limit the potential geographical distribution of *C. songaricum* and its host plants; (4) Quantifying the spatiotemporal evolution characteristics of the suitable area range under climate scenarios from SSP1-2.6 to SSP5-8.5 (2041–2060 and 2061–2080). By analyzing the impact mechanism of climate change on species distribution in different periods, the research results provide scientific basis for the introduction and cultivation of *C. songaricum* and its host plants, resource protection, and sustainable utilization, especially laying a theoretical foundation for the formulation of climate adaptation management strategies for parasitic plant ecosystems in arid areas.

## Results

### Model accuracy evaluation

The evaluation accuracy for ANN, CTA, FDA, GAM, GBM, GLM, MARS, MaxEnt, RF, and SRE was computed. For *C. songaricum* and its host plants, the TSS values of RF, GBM, MaxEnt, MARS, and GLM exceeded 0.80, AUC values exceeded 0.9, and KAPPA values exceeded 0.7 (Fig. 1). Consequently, an ensemble model (EM) was constructed using these five models, with the most accurate model being selected based on their performance metrics. The EM achieved TSS values greater than 0.85, AUC values greater than 0.95, and KAPPA values greater than 0.75 for *C. songaricum* and its host plants. Therefore, the EM built using distinct high-precision models demonstrated higher fitting accuracy and lower fitting uncertainty. In other words, the predicted potential geographic distributions of *C. songaricum* and its hosts using the EM were highly reliable.

### Current potential geographical distributions of *C. songaricum* and its host plants

The current potential geographic distributions of *C. songaricum* and its host plants, as estimated using EM, are shown in Fig. 2. The largest current suitable habitat area is that of *C. songaricum*, at $1710.91\times\times10^4$ km$^2$, followed by *Nitraria sibirica* ($1670.03\times10^4$ km$^2$), *Kalidium foliatum* ($1635.82\times10^4$ km$^2$), *N. tanguticum* ($955.55\times10^4$ km$^2$), *N. sphaerocarpa* ($807.36\times10^4$ km$^2$), *Zygophyllum xanthoxylum* ($665.00\times10^4$ km$^2$) and *Peganum multisectum* ($657.01\times10^4$ km$^2$) (Table S1). The potential geographic distribution of *C. songaricum* and its host plants is primarily centered in Asia. Highly suitable habitats for *C. songaricum* are mainly distributed in Asia (China, Mongolia) and North America (the United States) (Fig. 2A). Globally, the areas of highly suitable habitats for *C. songaricum* are approximately $372.70\times10^4$ km$^2$ (Table S1). China has the largest highly suitable habitat area for *C. songaricum*, followed by Mongolia and the United States (Table S1). Moderately suitable habitats for *C. songaricum* are primarily located around highly

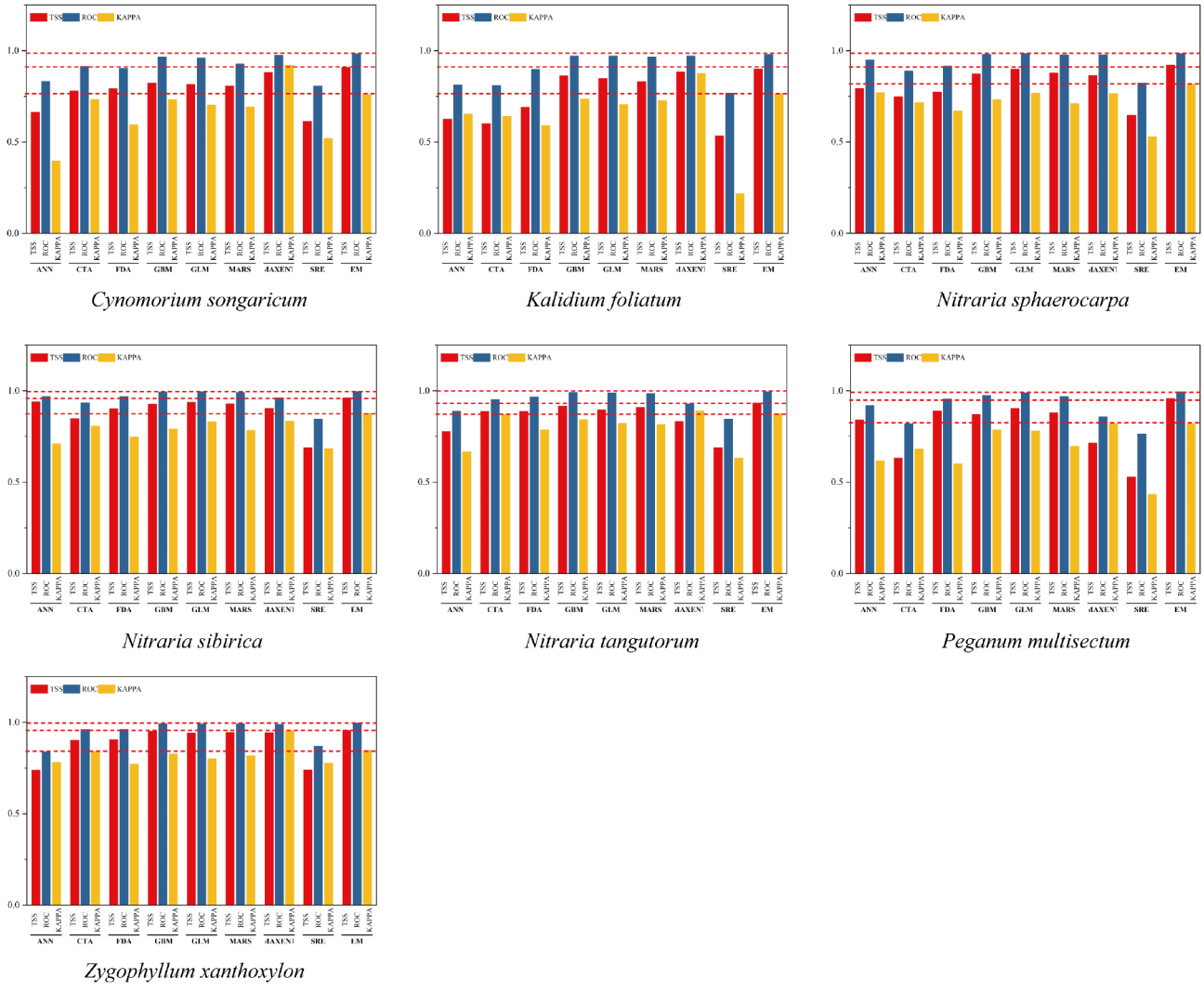


**Fig. 1** Accuracy evaluation results of different models

suitable habitats, and cover an area of $604.18 \times 10^4$ km$^2$ worldwide (Fig. 2A, Table S1).

Highly suitable habitats for *N. tangutorum* are primarily in Asia, with sporadic distributions in North America. The area of highly suitable habitat for *N. tangutorum* is approximately $280.20 \times 10^4$ km$^2$. Spanning an area of $344.95 \times 10^4$ km$^2$ globally, the moderately suitable habitats for *N. tangutorum* are predominantly located in proximity to highly suitable habitats (Fig. 2B, Table S1).

Highly suitable habitats for *N. sphaerocarpa* are primarily in Asia, with sporadic distributions in North America. The areas of highly suitable habitats for *N. sphaerocarpa* are approximately $151.88 \times 10^4$ km$^2$ worldwide. Moderately suitable habitats for *N. sphaerocarpa* are mainly distributed around highly suitable habitats, which cover an area of $151.88 \times 10^4$ km$^2$ km$^2$ worldwide (Fig. 2C, Table S2).

Highly suitable habitats for *N. sibirica* are predominantly found in Asia, spanning an area of approximately $393.47 \times 10^4$ km$^2$ globally. These habitats are surrounded by moderately suitable areas, which cover a total of $701.57 \times 10^4$ km$^2$ worldwide (Fig. 2D, Table S1).

Highly suitable habitats for *Peganum multisectum* are primarily situated in Asia, with occasional occurrences in North America. The global extent of these highly suitable habitats is around $288.74 \times 10^4$ km$^2$. Adjacent to these are the moderately suitable habitats, which collectively span an area of $316.77 \times 10^4$ km$^2$ globally (Fig. 2E, Table S1).

Highly suitable habitats for *Zygophyllum xanthoxylum* are primarily found in Asia, with occasional distributions in North America. The global expanse of these highly suitable habitats is approximately $260.50 \times 10^4$ km$^2$. Moderately suitable habitats for *Z. xanthoxylum* are typically proximate to the highly suitable ones, covering a global area of $232.65 \times 10^4$ km$^2$ (Fig. 2F, Table S1).

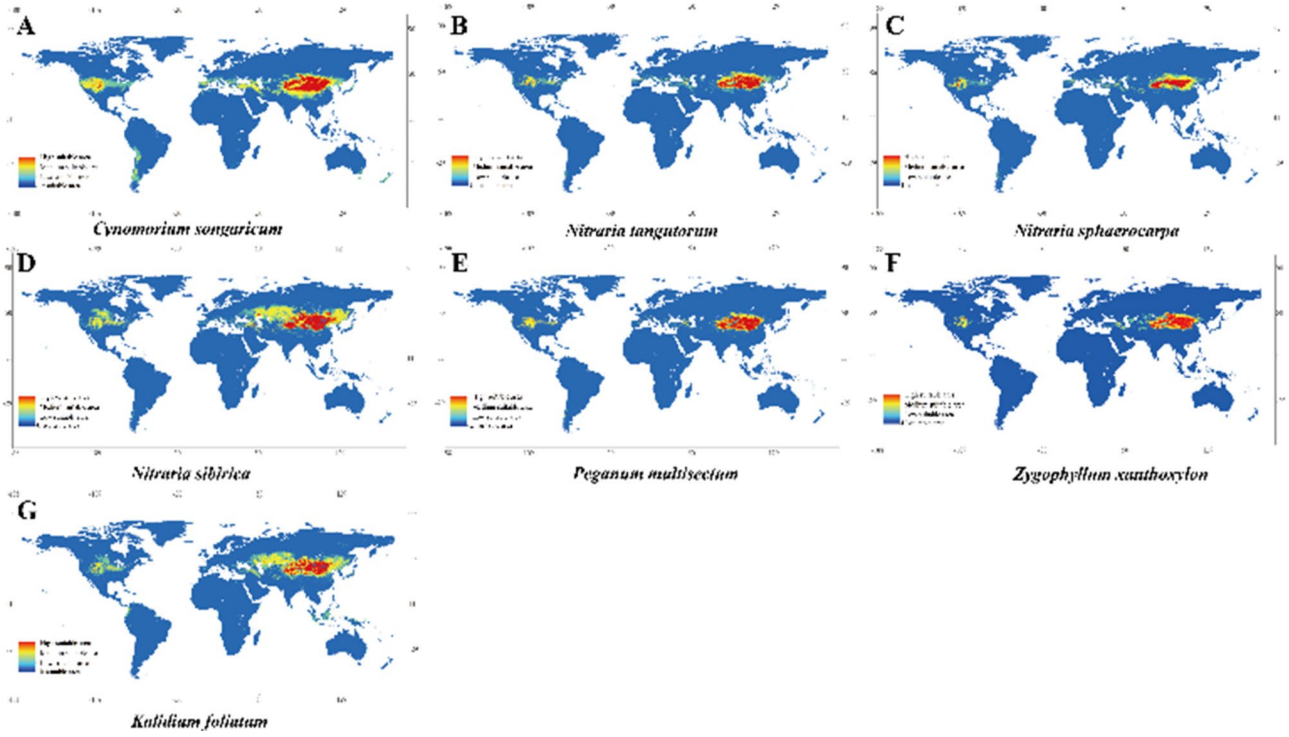


**Fig. 2** Current geographical distributions of Cynomorium songaricum (**A**), Nitraria tanguticum (**B**), N.sphaerocarpa (**C**), N.sibirica (**D**), Peganum multisectum (**E**), Zygophyllum xanthoxylon (**F**), and Kalidium foliatum (**G**) predicted using EM

Highly suitable habitats for *Kalidium foliatum* are primarily found in Asia, with occasional occurrences in North America. These highly suitable habitats span an area of approximately $298.33 \times 10^4$ $km^2$ globally. The moderately suitable habitats for *K. foliatum* are mainly situated adjacent to these areas and cover a total of $595.86 \times 10^4$ $km^2$ worldwide (Fig. 2G, Table S1).

### Future potential geographical distributions of *C. songaricum* and its host plants

The potential geographical distributions of *C. songaricum* and its host plants under SSP126, SSP245, SSP370 and SSP585 from 2041 to 2060 and 2061–2080 are shown in Fig. 3, 4, 5, 6, 7, respectively. For *C. songaricum*, compared with the current climatic conditions, the overall area of suitable habitat is expected to decrease under all four scenarios across the two timeframes (2041–2060 and 2061–2080) (Fig. 3). The most significant reduction in suitable habitat area is expected under SSP585 from 2061 to 2080, followed by SSP370 in 2061–2080 and SSP585 in 2041–2060 (Table S1). Suitable habitats are anticipated to decline in Asia (China, Türkiye, Iran, and Afghanistan) and North America (the United States) (Fig. 4). The areas with high and moderate suitability are predicted to be the largest under SSP370 from 2061 to 2080. Conversely, both the total and moderately suitable habitat areas are expected to be the smallest under SSP258 from 2061 to 2080, while highly suitable habitat areas will be the least extensive under SSP245 during the same timeframe.

The total area of suitable habitat for *K. foliatum* is predicted to increase across all four scenarios during both 2041–2060 and 2061–2080. The area of expanded suitable habitat is projected to be greatest under SSP 585 from 2061 to 2080, followed by SSP370 from 2041 to 2060 and SSP245 from 2061 to 2080 (Fig. S1). Suitable habitats are expected to expand across Asia (China, Mongolia, Türkiye, and Kazakhstan) and North America (America) (Fig. S7). The total and moderately suitable habitat areas are projected to be greatest under SSP 585 from 2061 to 2080, whereas the area of highly suitable habitat is expected to be greatest under SSP 370 from 2041 to 2060. Conversely, the total and moderately suitable habitat areas are anticipated to be the smallest under SSP126 from 2061 to 2080 (Fig. S1, Table S1).

For *N. sibirica*, the total area of suitable habitat is expected to expand under all four scenarios in both 2041–2060 and 2061–2080 compared with the current climatic conditions (Fig. S2). The area of expanded suitable habitat is projected to be greatest under SSP585 from 2041 to 2060, followed by SSP370 and SSP245 during the same time. The number of suitable habitats is expected to increase across Asia (China and Türkiye) and North America (the United States) (Fig. S8). The total, high, and moderate suitability habitat areas are projected to be greatest under SSP585 from 2041 to 2060. Conversely,

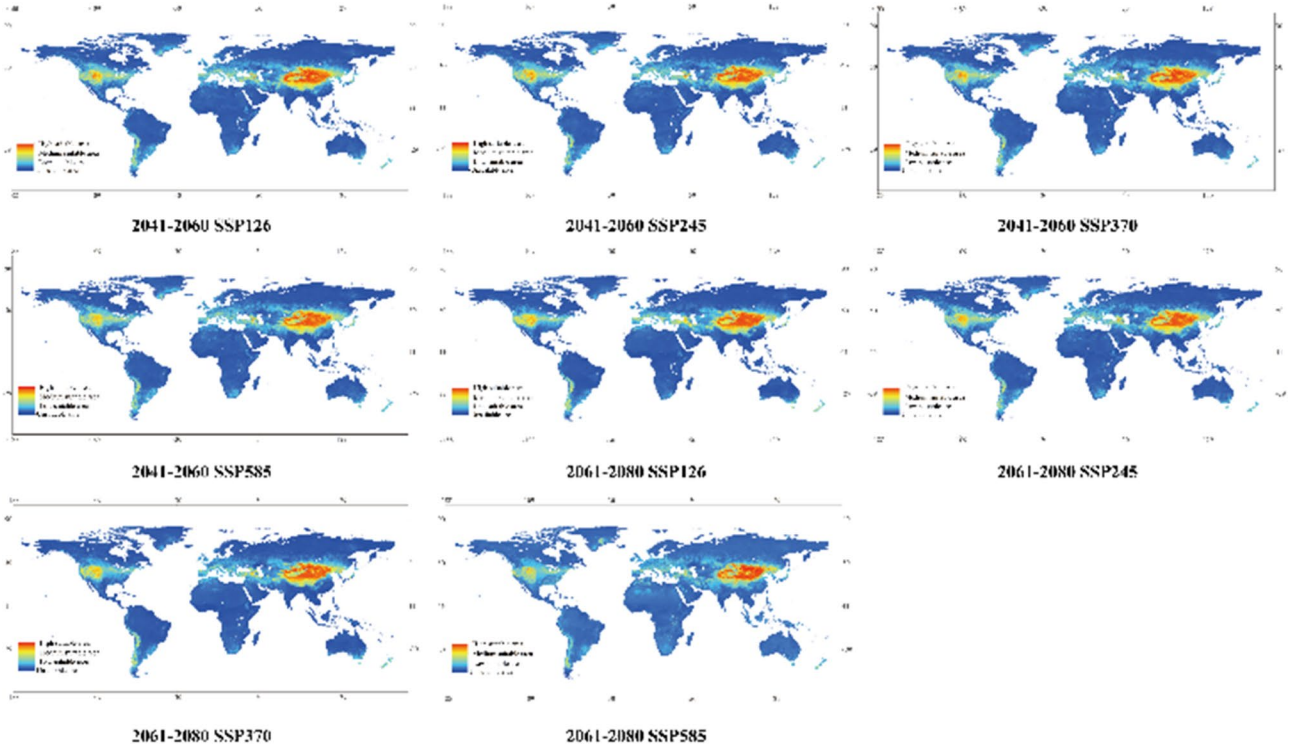


**Fig. 3** Averaged projected climatic suitability for *Cynomorium songaricum* in two timelines: 2041-60 and 2061-80 under four scenarios: SSP126, SSP245, SSP370, and SSP585

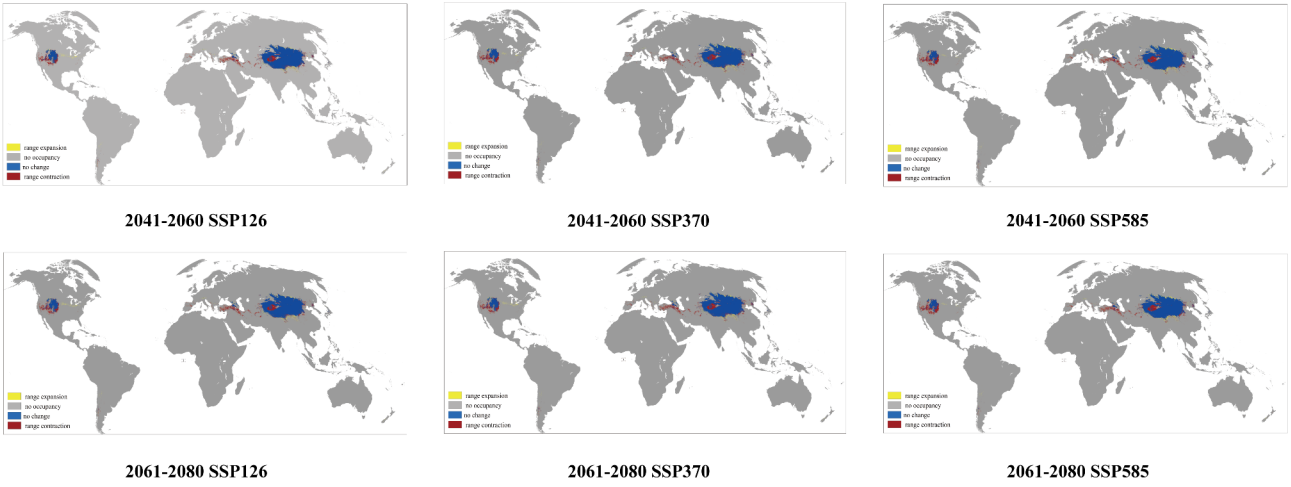


**Fig. 4** Averaged projected climatic suitability for *Cynomorium songaricum* in two timelines: 2041-2060 and 2061-2080 under three scenarios: SSP126, SSP370, and SSP585. For each timeline and scenario, we averaged output and discretised it over a predicted probability threshold to obtain a binary map, and then we compared it with current climatic suitability. Blue area indicates persistence (overlap of current and projected climatic suitability), red – future range contraction, yellow – future range expansion, grey – absence (unsuitable in both current and projected)

the total and highly suitable habitat areas are anticipated to be the smallest under SSP245 from 2061 to 2080, while the area of moderately suitable habitat is expected to be the least extensive under SSP370 from 2061 to 2080 (Fig. S2, Table S1).

For *N. sphaerocarpa*, the total area of suitable habitat is expected to decrease under all four scenarios in the both periods of 2041–2060 and 2061–2080 compared with the current climatic conditions (Fig. S3). The area of decreased suitable habitat is expected to be largest under SSP126 in 2061–2080, followed by SSP126 in 2041–2060. The number of suitable habitats is expected to decrease across Asia (China, Afghanistan, Iran, and Turkey) and North America (the United States) (Fig. S9).

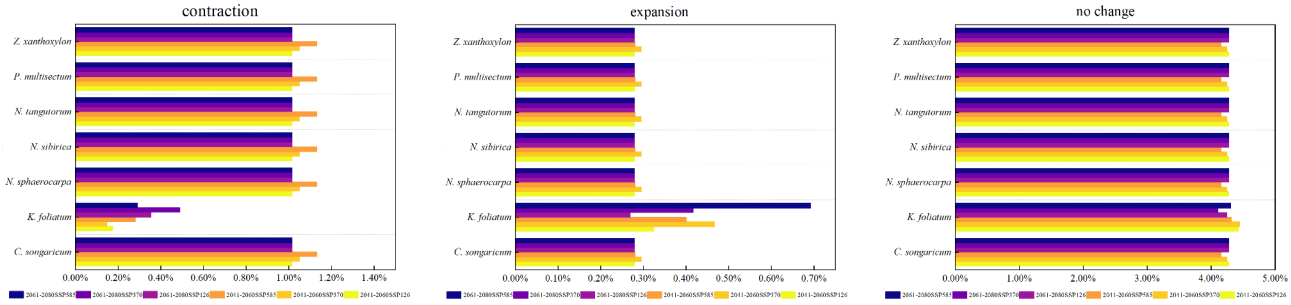


**Fig. 5** Proportion of range shifts of studied species under four climate change scenarios and two timelines

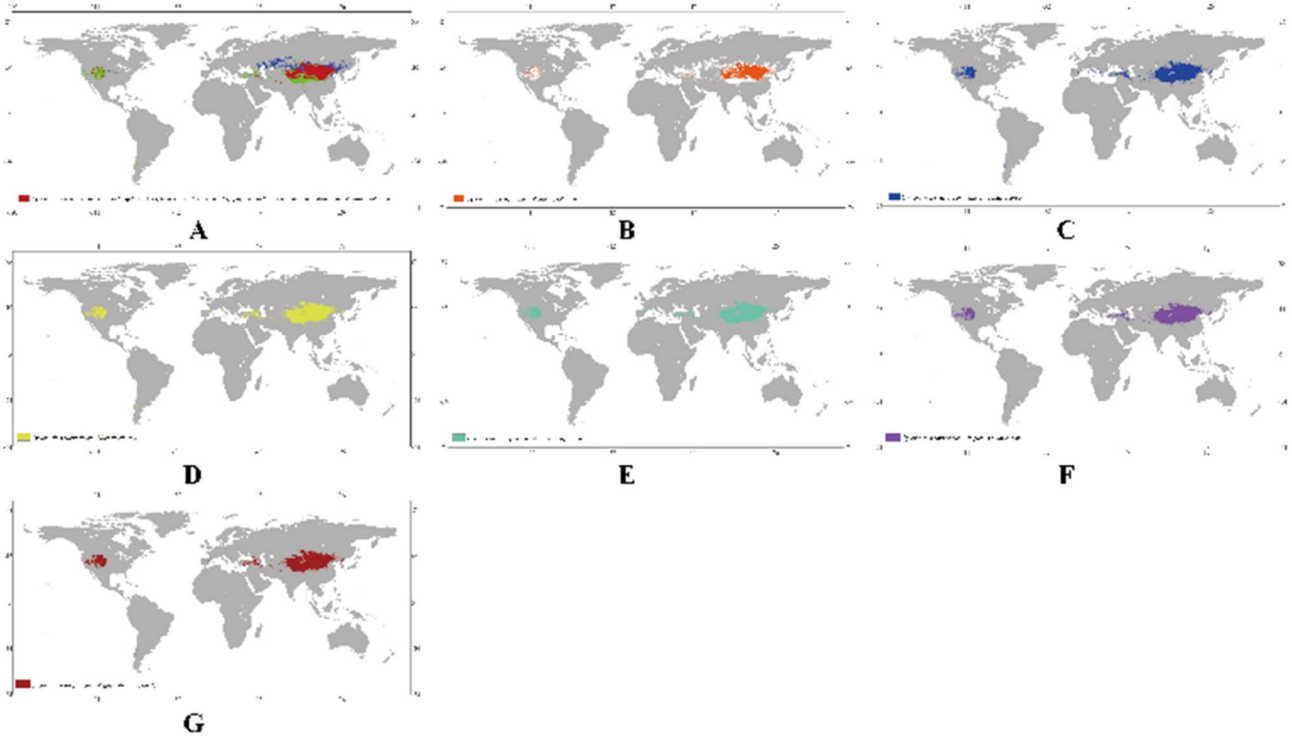


**Fig. 6** Overlapping geographical distribution areas of the Cynomorium songaricum and its host plants. (**A**) Cynomorium songaricum +Nitraria tangutorum+N.sphaerocarpa+N.sibirica+Zygophyllum xanthoxylon+Peganum multisectum +Kalidium foliatum; (**B**) C. songaricum+ K. foliatum; (**C**) C. songaricum+ N.sphaerocarpa; (**D**) C. songaricum+ N. sibirica; (**E**) C. songaricum+ N. tangutorum; (**F**) C. songaricum+ P. multisectum; (**G**) C. songaricum+ Z. xanthoxylon

The total, high, and moderate suitability habitat areas are projected to be greatest under SSP585 from 2041 to 2060. Conversely, the highly suitable habitat areas are expected to be the smallest under SSP 370 from 2061 to 2080, while the area of highly and moderately suitable habitat is expected to be the least extensive under SSP126 from 2041 to 2060 (Fig. S3, Table S1).

For *N. tanguticum*, the total area of suitable habitat is expected to contract under all four scenarios in both periods of 2041–2060 and 2061–2080 compared to the current climatic conditions (Fig. S4). The area of decreased suitable habitat is expected to be largest under SSP245 in 2061–2080, followed by SSP 370 and SSP585 during the same time. Suitable habitats are projected to decline across Asia (including China, Afghanistan, Iran, and Turkey) and North America (the United States) (Fig. S10). The total suitable habitat area is projected to be greatest under SSP585 from 2041 to 2060, whereas the high- and moderate-suitability habitat areas are expected to be greatest under SSP370 from 2041 to 2060 and 2061–2080, respectively. The total suitable habitat area would be the smallest under SSP245 from 2041 – 260, whereas the high- and moderate-suitability habitat areas would be the smallest under SSP370 from 2061 to 2080 and SSP245 from 2041 to 2060, respectively.

With respect to *P. multisectum*, the total area of suitable habitat is anticipated to decline under all four scenarios during both 2041–2060 and 2061–2080 compared

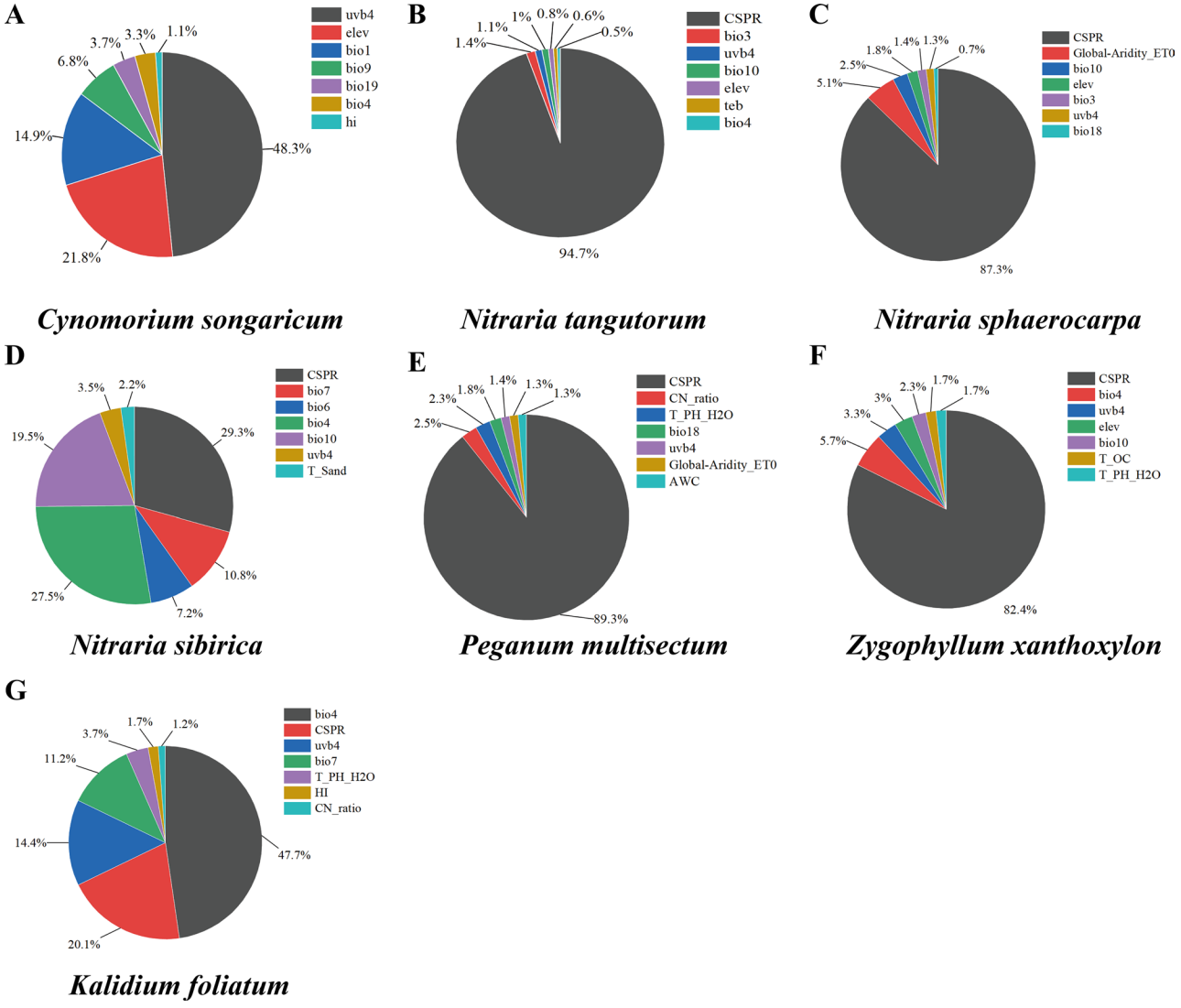


**Fig. 7** Importance of various environmental variables on *Cynomorium songaricum* and its host plants

with the current climatic conditions (Fig. S5). The area of reduced suitable habitat is projected to be greatest under SSP585 during the period of 2061–2080, followed by SSP126 within the same time. The number of suitable habitats is expected to decrease across Asia (including China, Afghanistan, Iran, and Turkey) and North America (the United States) (Fig. S11). The total area of suitable habitat is projected to be greatest under SSP126 from 2041 to 2060, whereas the areas of high and moderate suitability are expected to be greatest under SSP370 and SSP126 from 2041 to 2060, respectively.

For *Z. xanthoxylum*, the total area of suitable habitat is expected to expand under all four scenarios during both 2041–2060 and 2061–2080 compared with the current climatic conditions (Fig. S6). The area of expanded suitable habitat is projected to be greatest under SSP370 from 2061 to 2080, followed by SSP370 and SSP585 from 2041 to 2060. The number of suitable habitats is expected to increase across Asia (China and Mongolia) and North America (the United States) (Fig. S12). The high-suitability habitat areas are projected to be greatest under SSP585 from 2041 to 2060. Conversely, the total and moderately suitable habitat areas are expected to be the smallest under SSP126 from 2061 to 2080, while the area of highly suitable habitat is expected to be the smallest under SSP585 from 2061 to 2080.

### Range contraction and expansion

Each species, SSP scenario, and time period (2041–2060 and 2061–2080) exhibit distinct percentage values for range contraction, expansion, and persistence (Fig. 5). In general, all species except *K. foliatum* are projected to experience greater declines between 2041 and 2060 compared to the period from 2061 to 2080, particularly under

more severe climate change scenarios. Occupation values for the later period will be higher for all species except *K. foliatum*. For all species except *K. foliatum*, the extent of range expansion is similar between the two periods. However, *K. foliatum* is expected to acquire more suitable areas for colonization during 2061–2080 compared to 2041–2060.

### The ecological niches of *C. songaricum* and its host plants

*C. songaricum* and *K. foliatum* exhibited the broadest ecological niches, as evidenced by their highest B1 (0.2079 and 0.2344, respectively) and B2 (0.9293 and 0.9290, respectively) values, whereas *N. sphaerocarpa* exhibited the narrowest niches, with B1 and B2 values of 0.0821 and 0.8826, respectively. Furthermore, under alternative climate scenarios, the B1 and B2 values for *C. songaricum*, *N. sphaerocarpa*, *N. tangutorum*, and *P. multisectum* were lower than those in the current period (Table S2).

A high degree of ecological niche overlap was observed between *C. songaricum* and *N. sphaerocarpa*, as well as between *N. tangutorum* and *P. multisectum*, as indicated by both the D (D > 0.65) and I (I > 0.8) indices (Table 1). While these four species may share certain ecological niches, they are not identical. Range coverage analysis revealed that *C. songaricum* and *P. multisectum* had the highest range coverage (0.8747), followed by *Z. xanthoxylon* (0.7419) (Table 2), while *C. songaricum* and *K. foliatum* had the lowest range coverage (0.4457).

### Overlapping geographical distribution areas of *C. songaricum and* its host plants under climate change

The geographical areas where *C. songaricum* and its host plants overlap are predominantly distributed in Asia and North America (Fig. 6), encompassing an area of approximately $421.71 \times 10^4$ km$^2$. Among these, the overlap between *C. songaricum* and *K. foliatum* is the smallest, whereas the overlaps between *C. songaricum* and *N. tangutorum*, *N. sphaerocarpa*, *N. sibirica*, *Z. xanthoxylon*, and *P. multisectum* are each approximately $710.40 \times 10^4$ km$^2$.

### Impact of environmental variables on potential geographical distributions of *C. songaricum* and its host plants

Employing EM, the relative contributions of all environmental variables were calculated, and an investigation was conducted into the factors influencing the potential geographic distributions of C. songaricum and its host plants. The mean contribution value of each environmental variable is presented in Fig. S13. The cumulative contribution value of the ultraviolet-B factor was the highest for *C. songaricum* at 0.349437, whereas the cumulative contribution values for the CSPR (the influence of

**Table 1** Niche overlap between *C. songaricum* and it host plants

| Species | Niche overlap | | | | | | | | | | | | | |
|---|---|---|---|---|---|---|---|---|---|---|---|---|---|---|
| | D | | | | | | | I | | | | | | |
| | *Cynomorium songaricum* | *Nitraria tangutorum* | *N. sphaerocarpa* | *N. sibirica* | *Zygophyllum xanthoxylon* | *Peganum multisectum* | *Kalidium foliatum* | *Cynomorium songaricum* | *Nitraria tangutorum* | *N. sphaerocarpa* | *N. sibirica* | *Zygophyllum xanthoxylon* | *Peganum multisectum* | *Kalidium foliatum* |
| *Cynomorium songaricum* | | | | | | | | | | | | | | |
| *Nitraria tangutorum* | 0.6558 | | | | | | | 0.8743 | | | | | | |
| *N.sphaerocarpa* | 0.6783 | 0.4702 | | | | | | 0.8306 | 0.7872 | | | | | |
| *N.sibirica* | 0.5695 | 0.4864 | 0.4137 | | | | | 0.7888 | 0.7519 | 0.8788 | | | | |
| *Zygophyllum xanthoxylon* | 0.5503 | 0.5045 | 0.4860 | | | | | 0.7712 | 0.8416 | 0.8001 | 0.7181 | | | |
| *Peganum multisectum* | 0.6839 | 0.5194 | 0.4684 | 0.4408 | 0.5118 | | | 0.9351 | 0.8261 | 0.8360 | 0.7951 | 0.9000 | | |
| *Kalidium foliatum* | 0.5225 | 0.5525 | 0.5058 | 0.7086 | 0.5873 | 0.4321 | | 0.7682 | 0.8948 | 0.7110 | 0.7346 | 0.7264 | 0.8039 | |

**Table 2** Range overlap and niche breadth of *C. songaricum* and it host plants

| Species | Range overlap | | | | | | | Niche breadth | |
|---|---|---|---|---|---|---|---|---|---|
| | *Zygophyllum xanthoxylon* | *Cynomorium songaricum* | *Kalidium foliatum* | *Nitraria sibirica* | *N. sphaerocarpa* | *N. tangutorum* | *Peganum multisectum* | B1(inverse concentration) | B2(uncertainty) |
| *Zygophyllum xanthoxylon* | | | | | | | | 0.1034 | 0.8935 |
| *Cynomorium songaricum* | 0.7149 | | | | | | | 0.2079 | 0.9293 |
| *Kalidium foliatum* | 0.5386 | 0.4457 | | | | | | 0.2344 | 0.9290 |
| *Nitraria sibirica* | 0.9325 | 0.6392 | 0.4516 | | | | | 0.2157 | 0.8627 |
| *N. sphaerocarpa* | 0.4842 | 0.6225 | 0.8286 | 0.5800 | | | | 0.0821 | 0.8826 |
| *N. tangutorum* | 0.4081 | 0.5325 | 0.7237 | 0.5364 | 0.7729 | | | 0.1368 | 0.8609 |
| *Peganum multisectum* | 0.6686 | 0.8747 | 0.5640 | 0.7249 | 0.3608 | 0.3658 | | 0.0743 | 0.9092 |

the host plant on parasitic organisms) were the highest for *N. tangutorum*, *N. sphaerocarpa*, *Z. xanthoxylon* and *P. multisectum* at 0.8954, 0.7268, 0.5192 and 0.8701, respectively. The mean ultraviolet-B of the lowest month (UVB4, 48.3%), altitude (elev, 21.8%), and annual mean temperature (bio1, 14.9%) were the three environmental factors associated with *C. songaricum* with the highest contribution values (Fig. 7A).

The response curve illustrated the quantitative relationship between the logistic probability of presence and the suitable ranges of environmental variables (Fig. 8). For habitats with appropriate conditions, a threshold of ≥ 0.3 was selected for the main bioclimatic parameters, as plants thrive under these conditions. Specifically: - For *C. songaricum*, the suitable ranges were: UVB4: 2.05–1400 J/m$^2$/day, Elevation: 1116–2929 m, Bio1 (Annual Mean Temperature): 7.86–19.25 °C (Fig. 8A-C). For *N. tangutorum*, the suitable ranges were: Bio3 (Isothermality): 2.18–4611.174 J/m$^2$/day, Bio10 (Mean Temperature of Warmest Quarter): 11.1–28.3 °C (Fig. 8D-F). For *N. sphaerocarpa*, the suitable ranges were: Global-Aridity_ET0: 15887.27–18535.15, Bio10 (Mean Temperature of Warmest Quarter): 9–28 °C, Elevation: 2277.23–4676.61 m (Fig. 8G-I). For *N. sibirica*, the suitable ranges were: Bio4 (Temperature Seasonality): 1001.63–1724.88, Bio10 (Mean Temperature of Warmest Quarter): 13.62–32.11 °C, Bio7 (Temperature Annual Range): 7.7–54.69 °C (Fig. 8J-L). For *P. multisectum*, the suitable ranges were: CN_ratio: 4.05–15.95, Bio18 (Precipitation of Warmest Quarter): 111.76–251.45 mm, UVB4: 2.10–3023.32 J/m$^2$/day (Fig. 8M-O). For Z. xanthoxylon, the suitable ranges were: Bio4 (Temperature Seasonality): 750.34–818.72, UVB4: 68.97–1211.59 J/m$^2$/day, Elevation: 159.27–2966.35 m (Fig. 8P-R). For *K. foliatum*, the suitable ranges were: Bio4 (Temperature Seasonality): 902.75–1734.22, UVB4: 76.03–5872.05 J/m$^2$/day, Bio7 (Temperature Annual Range): 1–43.99 °C (Fig. 8S-U).

## Discussion

This study presents species distribution models for *C. songaricum* and its host plants, which are ecologically significant desert species. These results constitute the first comprehensive findings for *C. songaricum* and its host plants in China and neighbouring countries. Previous studies by Shao et al. (2022) [33] and He et al. (2021) [34] focused on other parasitic medicinal plants but examined only a single host species. Moreover, we utilized the Shared Socioeconomic Pathways (SSPs) from the IPCC Sixth Assessment Report to model potential distribution changes. Four SSPs were considered to estimate uncertainty in range shifts: SSP126 (sustainability, representing the most optimistic scenario aligned with RCP2.6 from the 5th report), SSP245 (a moderate scenario reflecting RCP4.5), SSP370 (regional rivalry, not included in the 5th report), and SSP485 (fossil fuel-driven development or business-as-usual, corresponding to RCP8.5). Additionally, future climate simulations from BCC-CSM2-MR

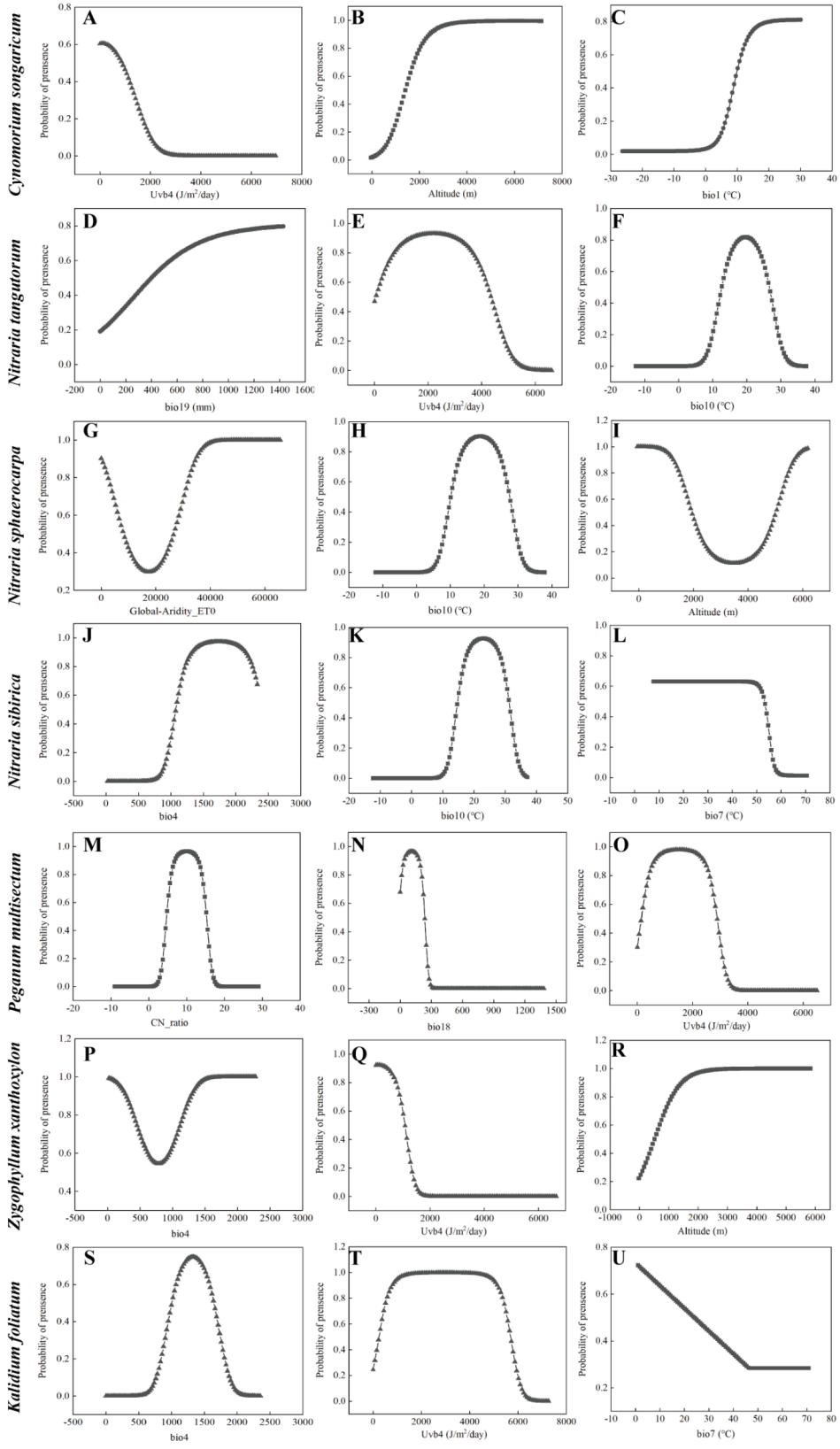


**Fig. 8** Response curves for dominant environmental variables in the species distribution model for *Cynomorium songaricum* and its host plants

(China), MRI-ESM2-0 (Japan), CanESM5 (Canada), and IPSL-CM6A-LR (France) were employed to reduce uncertainties associated with relying on a single model.

#### Data quality and study limitations

A multitude of species distribution models exist, and each is characterized by distinct focal points along with respective advantages and disadvantages. Consequently, achieving accurate predictive results using a singular model is challenging. Instead, integrating the prediction outputs from various models into an ensemble framework and establishing a weighted balance can significantly enhance predictive capabilities, effectively mitigate potential errors associated with reliance on a single model while facilitating more precise and reliable species distribution forecasts [54–56]. In terms of predicting suitable habitats for parasitic medicinal plants in China, this study employed a combined modelling approach as opposed to the sole MaxEnt model utilized by Shao et al. (2022) [33] and He et al. (2021) [34], which addresses issues related to the variability in ecological prediction inherent in current statistical methodologies [49]. Compared with those of the single model, the TSS, KAPPA, and AUC values of the combined model improved by 39.0% and 20.8% over those derived from the SRE model.

Some factors within the WorldClim data [57] exhibit a high degree of correlation, which might exert an adverse influence on the modelling outcomes [58]. In this study, the Pearson correlation coefficient and variance inflation factor (VIF) were comprehensively employed to reduce the dimensionality of the environmental data extracted from the actual occurrence points, which effectively addresses this issue [60–61]. Furthermore, when species distribution data are deficient and fail to cover the entire extent of species existence, it is termed incomplete sampling [62–63] and thereby augments the uncertainty of the model results. To mitigate the bias and uncertainty caused by such incomplete sampling, occurrence records for *C. songaricum* and its host plants since 1970 were collected. Once an occurrence record is identified, it can be presumed that the species still exists in the region. Consequently, species distribution data of *C. songaricum* and its host plants utilized in this study are complete, and the accuracy rate of the model constructed will be significantly enhanced.

Incorporating all range margins and systematically sampling every area within the occupied range are critical steps in developing species distribution models. The considerable overlap between the actual distribution and the current potential distribution for all investigated species (Fig. 2, Fig. S14), along with elevated TSS, AUC and KAPPA values (Fig. 1), implies a pronounced reliability of the models and satisfactory outcomes with respect to the trade-offs between the accuracy of occurrence data intended to mitigate sampling bias and the resolution of climate maps. Although our dataset does not uniformly encompass the entire distribution range (the dataset for North America is missing) and sampling biases cannot be entirely eradicated, our models for the current potential distribution of species exhibit considerable robustness. Consequently, we postulate that these findings provide a solid foundation for forecasting the potential distributions of the studied species under future climatic circumstances.

Simulations of potential habitats for its host plants conducted in this study provide a significant reference point for understanding the responses of desert ecosystems to climate change. Nevertheless, several factors may influence our findings. First, the precision and comprehensiveness of species occurrence data can significantly impact model certainty [64]. Although integrating data from multiple sources is increasingly recognized as a potential remedy [65–67], this approach can be challenging due to substantial differences among data sources in terms of assumptions, design, environmental coverage, and sampling biases [66, 66–68]. Second, model certainty may be influenced by uncertainties and limitations inherent in the biomod2 framework, particularly those related to pseudoabsence data and variability in environmental variables. For instance, the subjective nature of pseudoabsence point selection can lead to spatial biases, potentially misrepresenting species-environment relationships. Additionally, inadequate representation of habitat accessibility thresholds in pseudoabsence data may systematically overestimate potential distributions. The sensitivity of model outputs to pseudoabsence parameters, such as density ratios relative to presence points, underscores the need for rigorous sensitivity analyses. To address these limitations, we recommend implementing the following methodological refinements: (1) conducting systematic sensitivity analyses comparing targeted versus randomized pseudoabsence sampling approaches; (2) optimizing presence-pseudoabsence ratios through ROC curve and TSS evaluation to balance model specificity and sensitivity; (3) incorporating spatial block cross-validation to mitigate geographical sampling bias propagation; (4) establishing ensemble model variance outputs to quantify algorithm-specific sensitivity to pseudoabsence configurations. Third, this study focused exclusively on the effects of abiotic factors and host-related factors on the distribution of *C. songaricum*. As a holoparasitic plant, the distribution of *C. songaricum* is also influenced by host-parasite commensalism and human factors.

### Environmental variables significantly affect the potential geographical distributions of *C. songaricum* and its host plants

Environmental factors exert multi-dimensional regulatory effects on the distribution and survival of *C. songaricum* and its host plants [69–74]. Studies have shown that ultraviolet-B radiation (UV-B), altitude, and annual average temperature are the core driving factors for the distribution of *C. songaricum*. Among them, the lowest monthly average UV-B intensity (contributing rate 48.3%) directly affects the parasitism success rate of *C. songaricum* through inhibiting the photoblastic germination mechanism of seeds, while the distribution of host plants is limited by the annual average temperature of 8–12°C and annual precipitation < 200 mm, which represents the threshold of a drought climate. The characteristics of sandy soil (pH 7.5–8.5, salt content < 0.3%) and high-altitude gradient (800–2500 m) provide key habitats for the *C. songaricum*-host symbiotic system. However, future climate warming (ssp585 scenario with a temperature increase of 4.2°C) may cause the suitable area of host plants to contract towards higher altitudes (each 100 m of elevation increase leads to an increase of 1.2°C in adaptability), and exacerbate the fragmentation of *C. songaricum* habitats (the high suitability area is expected to decrease by 30–45% from 2041 to 2080). In addition, the enhancement of UV-B radiation due to ozone layer depletion (+ 15–20%) may further inhibit the physiological activity of *C. songaricum*. To address these challenges, protected areas need to be established in stable climate regions such as the Qaidam Basin and the Alxa Plateau. Through sand barriers for sand fixation, artificial reseeding of host plants (density ≥ 5 plants/100m$^2$) and remote sensing monitoring, adaptive management strategies can be optimized.

### Priority protected areas of *C. songaricum* and its host plants

Based on the Biomod2 ensemble model and the analysis of niche overlap, the priority protected areas for *C. songaricum* and its host plants should focus on the climate stable zone in the arid regions of Northwest China and Central Asia. Specifically, these areas include the northern edge of the Tarim Basin in Xinjiang, the sandy areas of the Hexi Corridor in Gansu, the Alashan Plateau in Inner Mongolia, and the Kizil Kum Desert in southern Kazakhstan. These areas show high ecological suitability (AUC > 0.85) in the current and future climate scenarios (SSP1-2.6 to SSP5-8.5), and the overlap degree of the distribution of *C. songaricum* and its hosts (Schoener's D > 0.6) is significantly higher than that in other areas (Table 2).

### Conservation and management strategies for *C. songaricum* and its host plants

To cope with the shrinking of suitable habitats caused by future warming (it is projected that the area of high suitability zone for *C. songaricum* and *N. sphaerocarpa*, *N. tanguticum*, will decrease from 2041 to 2080), comprehensive protected areas need to be established in high-altitude sandy areas such as the Qaidam Basin and Alashan League as climate refuges. Grazing and land reclamation should be restricted, and the stability of the micro-environment in the sandy areas should be maintained through artificial reforestation of host plants (such as *N. sphaerocarpa* and *N. tanguticum*) and sand barrier afforestation techniques. At the same time, cross-border cooperation mechanisms (such as the joint protection agreement between China and Kazakhstan) are crucial for coordinating the conservation of the symbiotic system of *C. songaricum* and its host plants in the desert belt of Central Asia.

The management of priority protected areas should integrate in-situ conservation (such as drone monitoring of host coverage) with ex-situ conservation (such as artificial breeding bases in Hexi Corridor), and optimize the parasitism success rate based on experimental evidence that the root exudates of the host (such as solanaceous auxin) regulate the germination of the *C. songaricum* seeds (with a 30% increase in germination rate, $p < 0.01$) [75]. Future efforts should be intensified to enhance the research on the genome and stress resistance traits of *C. songaricum* and its hosts to improve the sustainability of conservation measures.

## Conclusions

This study employed the biomod2 ensemble modeling framework to systematically evaluate the potential distribution patterns of *C. songaricum* and its host plants under current and future climate scenarios. The results demonstrate that mean ultraviolet-B of lowest month, altitude, and the annual mean temperature are the primary drivers of species distribution of *C. songaricum*. Projections under four scenarios within the two timeframes (2041–2060 and 2061–2080) indicate the reduction in overall suitable habitats for *C. songaricum*, *N. tangutorum*, *N. sphaerocarpa*, and *P. multisectum*. Drawing upon the findings of this study, conservation priorities for safeguarding species with substantial medicinal and ecological significance should be prioritized as follows: (1) the priority protected areas for *C. songaricum* and its host plants should focus on the arid and semi-arid sandy lands in Northwest China and Central Asia, with a particular emphasis on protecting the symbiotic system of *C. songaricum* and its host plants. These areas should maintain their ecological functions through climate adaptability and artificial intervention measures. In

the future, cross-regional cooperation (such as the joint protected area of China and Kazakhstan) needs to be strengthened to address the cross-border impacts of climate change on desert ecosystems. While model ensemble techniques significantly reduced single-algorithm uncertainty (average AUC improvement of 0.15), biases in pseudo-absence selection and limitations in environmental variable resolution may still affect prediction accuracy. To improve predictive accuracy, more comprehensive approaches are necessary, such as systematically addressing these issues through the integration of multi-source data streams – including remote sensing datasets (e.g., Sentinel-2-derived vegetation indices), citizen science observations (iNaturalist records), and environmental DNA (eDNA) genomics – thereby enhancing spatial resolution and predictive accuracy while advancing ecological niche modeling methodologies.

## Materials and methods

### Occurrence records

The occurrence records of *C. songaricum*, *N. tangutorum*, *N. sphaerocarpa*, *N. sibirica*, *P. multisectum*, *Zygophyllum xanthoxylon and K. foliatum* were obtained from the following sources: (1) websites (Global Biodiversity Information Facility, GBIF, https://www.gbif.org/; Chin ese Virtual Herbarium databases, CVH, https://www.cvh.ac.cn/; Plant Science of China, http://www.iplant.cn/frps); and (2) a relevant literature search. Subsequently, any occurrence data lacking precise geographic information were excluded from the analysis (Fig. S14). Using ENMTools [76], the occurrence data were screened so that each 5 km×5 km raster contained just one distribution point. Finally, 136, 160, 85, 145, 43, 107 and 102 occurrence records were obtained for *C. songaricum*, *N. tangutorum*, *N. sphaerocarpa*, *N. sibirica*, *Zygophyllum xanthoxylon*, *P. multisectum and K. foliatum* (Tables S3-S4).

### Environmental variables

To model current species distribution patterns, 47 environmental factors, including 3 terrain variables, 19 bioclimatic variables, 16 soil variables, 6 UV-B radiation variables and 3 other variables, that affect the distributions of *C. songaricum* and its hosts were downloaded [77–81]. Bioclimatic variables with a spatial resolution of 2.5′ from the WorldClim 2.1 database were utilized ( https://www.worldclim.org/data/worldclim21.html) (Table S5), which was derived from monthly mean temperature and precipitation measurements [82] as predictors of possible species distributions. Large chorological and phenological studies frequently use these data, which are especially useful for estimating the effects of climate change [83–86]. Sixteen soil variables were downloaded from the Harmonized World Soil Database (version 1.2, https://www.fao.org/soils -portal/). Six UV-B radiation variables were obtained from the Helmholtz Centre for Environmental Research (https://www.ufz.de/gluv/index.php?en=32367).

On the basis of the 47 environmental factors listed above, we considered the significance of variables derived from the jackknife technique and quantitatively assessed how environmental factors affect the geographic distribution of *C. songaricum* and its host plants. To incorporate host factors into the distribution model of *C. songaricum*, host plants were utilized as a limiting factor in the parasite analysis. To verify the significance and correlation of environmental factors, we used the VIF and Pearson correlation coefficient. The environmental factors with correlations less than 0.7 and variance inflation factor (VIF) values less than 10 were initially screened. Spearman correlation analysis and multicollinear variance inflation factor (VIF) analysis were conducted on the point interpolation data in the R language. The reciprocal of tolerance is another name for the variance expansion factor or VIF. There is no multicollinearity between factors when the VIF < 10, there is multicollinearity between factors when 10 < VIF < 100, and there is serious interfactor multicollinearity when 100 < VIF.

The Intergovernmental Panel on Climate Change (IPCC) Sixth Assessment Report, which outlines Shared Socioeconomic Pathways (SSPs) [87], was employed to model potential distribution changes. Shared Socioeconomic Pathways (SSPs), representing a new generation of socioeconomic scenarios for climate research, unify the socioeconomic assumptions used across various research communities, thereby improving the consistency and reliability of climate projections. SSP represent a significant advancement over the Representative Concentration Pathways (RCP) scenarios. This new framework not only refines and updates the original RCP2.6, RCP4.5, RCP6.0, and RCP8.5 scenarios to SSP1-2.6, SSP2-4.5, SSP4-6.0, and SSP5-8.5, respectively, but also introduces additional emission pathways such as SSP1-1.9, SSP4-3.4, SSP5-3.4-OSS, and SSP3-7.0. Compared to the RCP2.6 scenario, the SSP1-2.6 scenario exhibits a smoother trajectory. Despite its higher initial emissions levels, reflecting actual greenhouse gas (GHG) emissions between 2007 and 2014 that were significantly higher than those predicted by RCP2.6, this scenario ultimately follows a more moderate long-term trend. This suggests that under SSP1-2.6, global efforts towards more effective and proactive emission reduction measures have led to a more stable development path. For the SSP2-4.5 scenario, it incorporates a greater proportion of non-CO2 greenhouse gases compared to RCP4.5. Consequently, the radiative forcing changes start from a higher baseline and exhibit a slower rate of decline throughout the projection period. This highlights the increased importance of non-$CO_2$

gases in climate change impacts, necessitating enhanced focus on their emission control. The SSP4-6.0 scenario diverges notably from RCP6.0, with $CO_2$ emissions peaking in 2050 rather than 2080. Although SSP4-6.0 includes higher levels of non-$CO_2$ emissions, these adverse effects are mitigated by the assumption of accelerated emission reductions and technological advancements. This underscores the critical role of innovation and societal transformation in addressing the complexities of climate change. Finally, the SSP5-8.5 scenario portrays a high-emission future characterized by continuous increases in GHG emissions, leading to substantial global temperature rises. This scenario serves as a stark reminder that without effective mitigation actions, the risks associated with climate change could become even more severe. In summary, the SSP framework builds upon and extends the core concepts of the RCP scenarios by integrating socio-economic dimensions into climate modeling. This provides a more comprehensive and nuanced scenario structure for climate change research, which is essential for developing robust strategies and policies to mitigate climate change impacts. Four SSPs, SSP126 (sustainability, the most optimistic scenario reflecting RCP2.6 from the 5th report), SSP245 (a middle of the road, moderate scenario reflecting RCP4.5), SSP370 (regional rivalry, not used in the 5th report), and SSP485 (fossil fuel-based development or business-as-usual, reflecting RCP8.5), were considered to estimate the uncertainty of range shifts. Furthermore, every SSP was examined using four global circulation models (GCMs) as follows: BCC-CSM2-MR (China), MRI-ESM2-0 (Japan), CanESM5 (Canada), and IPSL-CM6A-LR (France). For all four SSPs, this amounts to half of the GCMs that are available. To consider the variability of GCMs, we chose to use randomly selected GCMs from different nations. To draw conclusions about the dynamics of species distribution shifts, we obtained future climatic data for two timelines as follows: 2041–2060 and 2061–2080.

#### Construction of the SDM and evaluation of model accuracy

Using an ecological niche modelling approach, we forecasted the habitat suitability of *C. songaricum* and its host plants under present and future climatic conditions. We used ensemble forecasting (EF), which creates a consensus model by applying multiple statistical algorithms [88]. Compared with individual models, this consensus model is thought to be a more reliable estimator [89].

Sillero (2011) [90] noted that integrating the outcomes of various methods, for example, methods based on disparate input data, can present problems. Generally, there are three types of models as follows: presence-only (such as climate envelope approaches), presence-absence (such as regression), and presence-background (such as the maximum entropy approach) models. Presence-absence models are better than presence-only models and presence-background approaches if accurate data on species absence are available. Therefore, we used the following nine presence–absence approaches from the algorithms implemented in the R package Biomod2 [91–92]: GLM—generalized linear models; GBM—generalized boosted models; ANN—artificial neuronal networks; SRE—surface range envelope; FDA—flexible discriminant analysis; MARS—multiple adaptive regression splines; RF—random forest; MAXENT—maximum entropy models; and CTA—classification and regression tree analysis.

Pseudoabsence data are generated from the initial background outside the occurrence points by the "random" parameter in the Biomod2 software. Two thousand pseudoabsence points are randomly generated each time and this process is repeated 3 times. To prevent the model from biasing towards a particular category during training, weights of the occurrence points and pseudoabsence points are adjusted so that the weighted sum of the two is equal. In this study, the "data. split. Theperc = 80" parameter is set in the Biomod2 software package to select 80% of the dataset containing occurrence points and pseudoabsence points as the training set and the remaining 20% as the test set. The division of the training and testing data was repeated 2 times. Each model performs one modelling operation on each group of pseudoabsence data and generates a total of 36 ($2 \times 2 \times 9$) predictive models.

The single algorithm parameters listed below were used to run the models. We used a stepwise feature selection process with quadratic terms based on the Akaike Information Criterion (AIC) to create the GLM. To guarantee fitting, GBM was conducted with a maximum of 2000 trees, a minimum of 10 observations in the terminal nodes of the trees, a learning rate of 0.01 and an interaction depth of 7. We employed a logit link function and a binomial distribution for the GAM. We set the initial random weights on [– 0.1, 0.1] with a maximum of 200 iterations, and we employed five cross-validations to determine the optimal size and decay parameters for the ANN. Using the MARS method, flexible discriminant analysis (FDA) was conducted. Five hundred trees and a node size of five were used when applying the RF. MAXENT was conducted with 1000 maximum iterations and a lq2lqptthreshold of 80. SRE was conducted with a quant of 0.025.

The accuracy of each individual model was evaluated using receiver operating characteristic (ROC) curves, true skill statistic (TSS) [93], and Kappa values [94]. TSS calculates the net prediction success rate of the model by utilizing presence and pseudo-absence points. The TSS value ranges from – 1 to 1; a TSS value closer to 1 indicates higher prediction accuracy, while a value closer to -1 suggests a more stochastic model. The area under

the ROC curve (AUC) is another criterion for assessing model performance, with an AUC > 0.95 indicating excellent model performance. Kappa statistics measure the agreement between predicted and observed outcomes relative to random chance, with a Kappa > 0.75 indicating excellent model performance [95]. Generally, higher values of these three metrics suggest greater model accuracy. Based on the evaluation results of individual models, those with TSS values greater than 0.7 and AUC values greater than 0.8 were selected to construct the ensemble model. Weights for each individual model in the ensemble were assigned based on their respective TSS scores, ensuring that models with higher TSS values received greater weight. This process ultimately yields combined model results for both current conditions and various future scenarios [96–97].

The Biomod_EnsembleModelling function adopts the em.algo parameter to choose from nine methods for integrated modelling. The options include EMmean (based on the probability mean of the selected model), EMmedian (based on the median probability of the selected model), EMwmean (based on the evaluation score), EMca (based on the binary voting of the selected model), EMci (based on the confidence interval around the probability mean of the selected model), and EMcv (based on the probability coefficient of variation in the selected model, i.e., SD/mean) with the selected model's probabilities weighted by the evaluation scores obtained at the time of model construction. Among these, EMmedian requires more memory and processing power than EMmean but is less affected by extreme anomalies. Instead of evaluating the probability of the occurrence of a species, EMmean can be used to evaluate uncertainty. In EMwmean, the weight in the subsequent integration increases with the quality of the prior model evaluation.

The appropriate integrated model was chosen after results of the Biomod _EnsembleForecasting function were assessed for TSS, ROC and KAPPA scores. Appropriate areas were categorized using the Jenks natural break classification (NBC) method. Following the development of the integrated model, distribution maps were normalized using ArcGIS 10.8, and the integrated model was projected onto the environmental variables for possible geographic distribution prediction using the Biomod _EnsembleForecasting function. Based on the results from Biomod2, 0-0.3, 0.3–0.5, 0.5–0.8, and 0.8-1 were the thresholds for unsuitable, low-suitable, medium-suitable, and high-suitable areas for *C. songaricum* and its host plants, respectively. Additionally, the SDM toolbox v 2.5 plug-in was used to calculate the distribution changes between the current period and each period of the future for *C. songaricum* and its host plants.

### Overlapping geographical distribution areas of *C. songaricum* and its host plants

Using ArcGIS 10.4 software, we first classified all possible geographical distributions of *C. songaricum* and its host plants with probabilities > 0.3 (the cut-off point between low suitability habitat and unsuitable habitat) as "suitable" and all those with probabilities less than 0.3 as "unsuitable" for the overlapping geographical distribution areas. The overlapping geographic distribution areas of *C. songaricum* and its host plants were subsequently superimposed on their suitable areas. Finally, the distribution area of *C. songaricum*, which is separately parasitic on its host plants, was identified on the basis of the overlapping geographical distribution areas of these species.

### Measurement of the ecological niche

Initially, the niche breadth of each species in geographic and environmental space was determined by calculating the mean Levins' B1 (inverse concentration) and B2 (uncertainty) values using ENMTools v1.3. The distribution of Levins' B1 and B2 values, which ranged from 0 to 1, revealed that higher values suggest greater niche width and that smaller values indicate confined niche breadth. Next, on the basis of the EM output, the ecological niche differences, including overlap and range overlap, between *C. songaricum* and its host plants were calculated using the ENMTools software. The ecological niche overlap test was used to compare the degree of ecological niche overlap among *C. songaricum* and its host plants by measuring the similarities between their ecological niches using Schoener's D [98] and Hellinger's distance (I) [99]. Generally, the values of D and I varied from 0 (signifying a minimal level of overlap in niches) to 1 (signifying a significant level of overlap in niches). Finally, ArcGIS was used to visualize the overlapping zones, which included the highly and moderately suitable habitats of paired species to support the hypothesis.

## Supplementary Information

The online version contains supplementary material available at https://doi.org/10.1186/s12870-025-06370-8.

Supplementary Material 1
Supplementary Material 2
Supplementary Material 3
Supplementary Material 4
Supplementary Material 5
Supplementary Material 6
Supplementary Material 7
Supplementary Material 8
Supplementary Material 9

Supplementary Material 10

Supplementary Material 11

Supplementary Material 12

Supplementary Material 13

Supplementary Material 14

Supplementary Material 15

Supplementary Material 16

Supplementary Material 17

Supplementary Material 18

Supplementary Material 19

**Author contributions**
Yang LC wrote the main manuscript text, Jia HM prepared Figs. 1, 2 and 3, and Hua Q collected data. All authors reviewed the manuscript.

**Funding**
This study was supported by the Open Project of Qinghai Key Laboratory of Qinghai-Tibet Plateau Biological Resources.

**Data availability**
The data presented in this article and the Supplementary Information were sourced from the following databases: the Global Biodiversity Information Facility (GBIF, https://www.gbif.org/), the Chinese Virtual Herbarium (http://www.cvh.ac.cn/), the China National Specimen Information Infrastructure (http://www.naii.org.cn), WorldClim (http://worldclim.org), and the National Tibetan Plateau Data Center (https://data.tpdc.ac.cn/zh-hans/). The raw data of this article will be made available by corresponding authors, according to the personal requests.

## Declarations

**Ethics approval and consent to participate**
This study including the collection of plant samples complies with relevant institutional, national, and international guidelines and legislation. All the necessary permissions have been granted for this research.

**Consent for publication**
Not applicable.

**Competing interests**
The authors declare no competing interests.

**Author details**
[1]Qinghai Province Key Laboratory of Qinghai-Tibet Plateau Biological Resources, Northwest Institute of Plateau Biology, Chinese Academy of Sciences, Xining 810008, China
[2]Maqin County Yangyu Forest Farm, Maqin 814000, China
[3]Golog Tibetan Autonomous Prefecture Agriculture and Animal Husbandry Comprehensive Service Center, Maqin 814000, China

Received: 14 August 2024 / Accepted: 8 March 2025
Published online: 18 March 2025

**References**

1. Editorial Committee of the Flora of China, Chinese Academy of Sciences. Flora of China (No. 53 Vol. 2). Beijing: Science Press. 1999; 53(2):152–152.
2. Luo GH, Wang J, Yan X, Zhang Y, Zhang GX, Wang JQ. Differences of *Cynomorium songaricum* seed quality and mutual parasitism in different host plants. Chin J Chin Mater Med 2013;38(20):3432–3437. https://doi.org/10.4268/cjcmm20132005
3. Xie YL, Li XC, Xu JY, Jiang Q, Xie H, He JF, Chen DF. Two phenolic antioxidants in Suoyang enhance viability of •OH-damaged mesenchymal stem cells: comparison and mechanistic chemistry. Chem Cent J. 2017;11:84. https://doi.org/10.1186/s13065-017-0313-1.
4. Meng HC, Wang S, Li Y, Kuang YY, Ma CM. Chemical constituents and Pharmacologic actions of *Cynomorium* plants. Chin J Nat Med. 2013;11(4):321–9. https://doi.org/10.1016/S1875-5364(13)60049-7.
5. Wang XF, Li H, Liu MP, Jiao HS. Chemical constituents from *Cynomorium songaricum* Rupr. Chin Tradit Pat Med. 2015;37(8):1737–9.
6. Zhang WG, Zheng NN, Rui Y, Fan QN, Duan YF. Extraction technology and in vitro antioxidant activity of polysaccharide from wild of *Cynomorium songaricum* Rupr in Ningxia. Sci Technol Food Ind. 2014;35(24):279–84.
7. Ma JX, Li W, Yu XY. Correlation between HPLC fingerprints and anti - aging effect of *Cynomorium songaricum* Rupr. Chin J Clin Pharmacol. 2018;34(16):1982–5.
8. Ren MY, Yang G, Du LS, Liu F, Zhang D, Shen Q, Guan X, Zhang YD. Research advances in medicinal plants of *Cynomorium songaricum*. J Bio. 2018;35(5):95–8. https://doi.org/10.3969/j.issn.2095-1736.2018.05.095.
9. Chen Y, Han DH, Gao H, Luo GH, Wang J. Distribution and utilization on germplasm resources of host plants of cynomorium Songaricum. Chin Wild Plant Resou. 2013;32(5):45–7. https://doi.org/10.3969/j.issn.1006-9690.2013.05.011.
10. Han H, Cho S, Song J, Seol A, Chung H, Kim J, Chung J. Assessing the potential suitability of forest stands as *Kirengeshoma koreana* habitat using maxent. Landsc Ecol Eng. 2014;10:339–48. https://doi.org/10.1007/s11355-013-0246-3.
11. Ren MY, Yang G, Du LS, Liu F, Zhang D, Shen Q, Guan X, Zhang YD. Research advances in medicinal plants of *Cynomorium songaricum*. J Biol. 2018;35(5):95–8. https://doi.org/10.3969/j.issn.2095-1736.2018.05.095.
12. Zhang R, Gu ZR, Guo Y, Qi M, Lv X, Mao XW, Ge B. Content difference of effective components of cynomorii herba between different producing areas and its response to environmental factors. Chin J Exper Trad Med Form. 2022;28(7):142–50. https://doi.org/10.13422/j.cnki.syfjx.20220512.
13. Weiss AD. Topographic position and landforms analysis. Poster Presentation, ESRI Users Conference; 2001; San Diego, CA.
14. Groom MJ, Meffe BK, Carroll CR. Principles of Conservation Biology. 3rd ed. Sunderland, USA: Sinauer Associates, Inc. Publishers; 2006.
15. Pacifici M, Visconti P, Butchart SHM, Watson JEM, Cassola FM, Rondinini C. Author correction: species' traits influenced their response to recent climate change. Nat Clim Change. 2018;8:750. https://doi.org/10.1038/s41558-018-0229-3.
16. Moraitis ML, Valavanis VD, Karakassis I. Modelling the effects of climate change on the distribution of benthic indicator species in the Eastern mediterranean sea. Sci Total Environ. 2019;667:16–24. https://doi.org/10.1016/j.scitotenv.2019.02.338.
17. Franklin J. Species distribution models in conservation biogeography: developments and challenges. Divers Distrib. 2013;19:1217–23. https://doi.org/10.1111/ddi.12125.
18. Xu ZL, Peng HH, Peng SZ. The development and evaluation of species distribution models. Acta Ecol Sin. 2015;35(2):557–67. https://doi.org/10.5846/stxb201304030600.
19. Phillips SJ, Anderson RP, Schapire RE. Maximum entropy modeling of species geographic distributions. Ecol Model. 2006;190(3–4):231–59. https://doi.org/10.1016/j.ecolmodel.2005.03.026.
20. Breiman L. Random forests. Mach Learn. 2001;45:5–32.
21. McCulloch CE. Generalized linear models. J Am Stat Assoc. 2000;95(452):1320–4. https://doi.org/10.2307/2669780.
22. Zhao GH, Cui XY, Sun JJ, Li TT, Wang Q, Ye XZ, Fan BG. Analysis of the distribution pattern of Chinese Ziziphus Jujuba under climate change based on optimized Biomod2 and maxent models. Ecol Indic. 2021;132:108256. https://doi.org/10.1016/j.ecolind.2021.108256.
23. Thuiller W. BIOMOD – optimizing predictions of species distributions and projecting potential future shifts under global change. Glob Chang Biol. 2003;9:1353–62. https://doi.org/10.1046/j.1365-2486.2003.00666.x.
24. Thuiller W, Lafourcade B, Engler R, Araújo MB. BIOMOD-a platform for ensemble forecasting of species distributions. Ecography. 2009;32:369373. https://doi.org/10.1111/j.1600-0587.2008.05742.x.
25. Thuiller W, Araújo MB, Lavorel S. Generalized models vs. classification tree analysis: predicting Spatial distributions of plant species at different scales. J Veg Sci. 2003;14:669–80. https://doi.org/10.1111/j.1654-1103.2003.tb02199.x.
26. Huang DY, An QJ, Huang SP, Tan GD, Quan HG, Chen YE, Zhou JY, Liao H. Biomod2 modeling for predicting the potential ecological distribution of three *Fritillaria* species under climate change. Sci Rep. 2023;13:18801. https://doi.org/10.1038/s41598-023-45887-6.

27. Yang LC, Zhu XF, Song WZ, Shi XP, Huang XT. Predicting the potential distribution of 12 threatened medicinal plants on the Qinghai-Tibet plateau, with a maximum entropy model. Eco Evol. 2024;14:e11042. https://doi.org/10.1002/ece3.11042.
28. Song D, Li Z, Wang T, Qi Y, Han H, Chen Z. Prediction of changes to the suitable distribution area of *Fritillaria przewalskii* Maxim. In the Qinghai-Tibet plateau under shared socioeconomic pathways (SSPs). Sustainability. 2023;15:2833. https://doi.org/10.3390/su15032833.
29. Chen KY, WangB, Chen C, Zhou GY. MaxEnt modeling to predict the current and future distribution of *Pomatosace filicula* under climate change scenarios on the Qinghai-Tibet plateau. Plants. 2022;11:670. https://doi.org/10.3390/plants1105067013
30. Gao XX, Liu J, Huang ZH. The impact of climate change on the distribution of rare and endangered tree *Firmiana kwangsiensis* using the maxent modeling. Eco Evol. 2022;12(8):e9165. https://doi.org/10.1002/ece3.
31. Wang YJ, Zhao RX, Zhou XY, Zhang XL, Zhao GH, Zhang FG. Prediction of potential distribution areas and priority protected areas of *Agastache rugosa* based on maxent model and Marxan model. Front Plant Sci. 2023;14:1200796. https://doi.org/10.3389/fpls.2023.1200796.
32. Zhang H, Zhao HX. Study on rare and endangered plants under climate: maxent modeling for identifying hot spots in Northwest China. Cerne. 2021;27:e–102667. https://doi.org/10.1590/01047760202127012667.
33. Shao MH, Wang L, Li BW, Li SY, Fan JL, Li CJ. Maxent modeling for identifying the nature reserve of *Cistanche deserticola* Ma under effects of the host (*Haloxylon Bunge*) forest and climate changes in Xinjiang, China. Forests. 2022;13:189. https://doi.org/10.3390/f13020189.
34. He P, Li YF, Xu N, Peng C, Meng FY. Predicting the suitable habitats of parasitic desert species based on a niche model with *Haloxylon ammodendron* and *Cistanche deserticola* as examples. Eco Evol. 2021;11:17817–34. https://doi.org/10.1002/ece3.8340.
35. Nickrent DL. Parasitic angiosperms: how often and how many? Taxon. 2020;69(1):5–27. https://doi.org/10.1002/tax.12195.
36. Nickrent DL. Orígenes filogenéticos de Las Plantas Parásitas.Pp. 29–56. In: López-Sáez JA, Catalán P, Sáez L, editors. *Plantas parásitas de La Península ibérica e* Islas Baleares. Madrid: Mundi-Prensa Libros; 2002.
37. Moudrý V, Símoá P. Influence of positional accuracy, sample size and scale on modelling species distributions: a review. Int J Geogr Inf Sci. 2012;26(11):2083–95.
38. Pearson RG, Thuiller W, Araújo MB, Martinez-Meyer E, Brotons L, McClean C, Lees DC. Model-based uncertainty in species range prediction. J Biogeogr. 2006;33(10):1704–11.
39. Watling JI, Brandt LA, Bucklin DN, Fujisaki I, Mazzotti FJ, Romanach SS, Speroterra C. Performance metrics and variance partitioning reveal sources of uncertainty in species distribution models. Ecol Model. 2015;309:48–59.
40. Aguirre-Gutiérrez J, Carvalheiro LG, Polce C, van Loon EE, Raes N, Reemer M, Biesmeijer JC. Fit-for-purpose: species distribution model performance depends on evaluation criteria–Dutch hoverflies as a case study. PLoS ONE. 2013;8(5):e63708.
41. Dormann CF, Purschke O, García Márquez JR, Lautenbach S, Schröder S. Components of uncertainty in species distribution analysis: a case study of the great grey shrike. Ecology. 2008;89:3371–86.
42. Elith J, Graham HC, Anderson PR, Dudík M, Ferrier S, Guisan A, Li J. Novel methods improve prediction of species' distributions from occurrence data. Ecography. 2006;29(2):129–51.
43. Carvalho SB, Brito JC, Pressey RL, Crespo E, Possingham HP. Simulating the effects of using different types of species distribution data in reserve selection. Biol Conserv. 2010;143(2):426–38.
44. Mendes P, Velazco SJE, de Andrade AFA, Júnior PDM. Dealing with overprediction in species distribution models: how adding distance constraints can improve model accuracy. Ecol Model. 2020;431:109180.
45. Segurado P, Araujo MB. An evaluation of methods for modelling species distributions. J Biogeogr. 2004;31(10):1555–68.
46. Zhang YC, Jiang XH, Lei YX, Wu QL, Liu YH, Shi XW. Potentially suitable distribution areas of *Populus euphratica* and *Tamarix chinensis* by maxent and random forest model in the lower reaches of the Heihe river. China Environ Monit Assess. 2023;195:1519. https://doi.org/10.1007/s10661-023-12122-8.
47. Zhao GH, Cui XY, Sun JJ, Li TT, Wang Q, Ye XZ, Fan BG. Analysis of the distribution pattern of Chinese Ziziphus Jujuba under climate change based on optimized biomod2 and maxent models. Ecol Indic. 2021;132:108256.
48. Thuiller W, Lafourcade B, Engler R, Araújo MB. BIOMOD—A platform for ensemble forecasting of species distributions. Ecography. 2009;32:369–73.
49. Thuiller W, Biomod. Optimizing predictions of species distributions and projecting potential future shifts under global change. Glob Chang Biol. 2003;9:1353–136212.
50. Huang DY, An QJ, Huang SP, Tan GD, Quan HG, Chen YE, Zhou JY, Liao H. Biomod2 modeling for predicting the potential ecological distribution of three fritillaria species under climate change. Sci Rep. 2023;13:18801. https://doi.org/10.1038/s41598-023-45887-6.
51. Xian XQ, Zhao HX, Wang R, Huang HK, Chen BX, Zhang GF, Liu WX, Wan FH. Climate change has increased the global threats posed by three ragweeds (Ambrosia L.) in the anthropocene. Sci Total Environ. 2023;859:160252. https://doi.org/10.1016/j.scitotenv.2022.160252.
52. Jia T, Qi Y, Zhao H, Xian X, Li J, Huang H, Yu W, Liu W-X. Estimation of climate-induced increased risk of *Centaurea solstitialis* L. invasion in China: an integrated study based on biomod2. Front Ecol Evol. 2023;11:1113474. https://doi.org/10.3389/fevo.2023.1113474.
53. Luo M, Wang H, Lv Z. Evaluating the performance of species distribution models Biomod2 and maxent using the giant panda distribution data. Chin J Appl Ecol. 2017;28:4001–6.
54. Bi YF, Xu JC, Li QH, Guisan A, Thuiller W, Zimmermann NE, Yang YP, Yang XF. Applying biomod for Model-ensemble in species distributions: a case study for *Tsuga chinensis* in China. Plant Divers Resour. 2013;35(5):647–55. https://doi.org/10.7677/ynzwyj201312127.
55. Araújo MB, New M. Ensemble forecasting of species distributions. Trends Ecol Evol. 2007;22:42–7.
56. Zhao ZF, Guo YL, Wei HY, Ran Q, Liu J, Zhang QZ, Gu W. Potential distribution of *Notopterygium incisum* Ting ex H.T. Chang and its predicted responses to climate change based on a comprehensive habitat suitability model. Ecol Evol. 2020;10:3004–16. https://doi.org/10.1002/ece3.6117.
57. Fick SE, Hijmans RJ. WorldClim 2: new 1 Km Spatial resolution climate surfaces for global land areas. Int J Climatol. 2017;37:4302–431536.
58. Eyring V, Bony S, Meehl GA, Senior CA, Stevens B, Stouffer RJ, Taylor KE. Overview of the coupled model intercomparison project phase 6 (CMIP6) experimental design and organization. Geosci Model Dev. 2016;9(5):1937–58. https://doi.org/10.5194/gmd-9-1937-2016.
59. Guisan A, Thuiller W, Zimmermann NE. Habitat suitability and distribution models: with applications in R. Cambridge: Cambridge University Press; 2017.
60. Fourcade Y, Besnard AG, Secondi J. Paintings predict the distribution of species, or the challenge of selecting environmental predictors and evaluation statistics. Glob Ecol Biogeogr. 2018;27:245–56.
61. Albert CH, Yoccoz NG, Edwards JTC, Catherine H, Graham, Zimmermann NE, Thuiller. W.Sampling in ecology and evolution-bridging the gap between theory and practice. Ecography. 2010;33:1028–37. https://doi.org/10.1111/j.1600-0587.2010.06421.x.
62. Fei S, Yu F. Quality of presence data determines species distribution model performance: A novel index to evaluate data quality. Landsc Eco. 2015;31:31–42.
63. Rocchini D, Garzon-Lopez CX. Cartograms tool to represent Spatial uncertainty in species distribution. Res Ideas Outcomes. 2017;3:e12029. https://doi.org/10.3897/rio.3.e12029.
64. Xian XQ, Zhao HX, Wang R, Huang HK, Chen BX, Zhang GF, Liu WX, Wan FH. Climate change has increased the global threats posed by three ragweeds *(Ambrosia* L.) in the anthropocene. Sci Total Environ. 2023;859:160252. https://doi.org/10.1016/j.scitotenv.2022.160252.
65. Carvalho SB, Brito JC, Crespo EJ, Possingham HP. From climate change predictions to actions – conserving vulnerable animal groups in hotspots at a regional scale. Glob Chang Biol. 2010;16:3257–70. https://doi.org/10.1111/j.1365-2486.2010.02212.xr2010.
66. Fletcher RJ Jr, Hefley TJ, Robertson EP, Zuckerberg B, McCleery RA, Dorazio RM. Ecology. 2019;100(6):e02710. https://doi.org/10.1002/ecy.2710. A practic al guide for combining data to model species distributions.
67. Isaac NJB, Jarzyna MA, Keil P, Dambly LI, Boersch-Supan PH, Browning E, Freeman SN, Golding N, Guillera-Arroita G, Henrys PA, Jarvis S, Lahoz-Monfort J, Pagel J, Pescott OL, Schmucki R, Simmonds EG, O'Hara RB. Trends Ecol Evol. 2020;35:56–67. https://doi.org/10.1016/j.tree.2019.08.006. Data integration for large-scale models of species distributions.
68. Pacifici M, Visconti P, Butchart SHM, Watson JEM, Cassola FM, Rondinini C. Species' traits influenced their response to recent climate change. Nat Clim Change. 2017;7:205208. https://doi.org/10.1038/nclimate3223.
69. Anibaba QA, Dyderski M, Jagodzi´nski AM. Predicted range shifts of invasive giant hogweed (*Heracleum mantegazzianum*) in Europe. Sci Total Environ. 2022;825:154053. https://doi.org/10.1016/j.scitotenv.2022.154053.

70. Olszewski P, Dyderski M, Dylewski Ł, Bogusch P, Schmid-Egger C, Ljubomirov T, Zimmermann D, Le Divelec R, Wiśniowski B, Twerd L, Pawlikowski T, Mei M, Popa AF, Szczypek J, Sparks TH, Puchałka R. European Beewolf (*Philanthus triangulum*) will expand its geographic range as a result of climate warming. Reg Environ Chang. 2022;22:129. https://doi.org/10.1007/s10113-022-01987-z.
71. Puchałka R, Dyderski M, Vítková M, Sádlo J, Klisz M, Netsvetov M, Prokopuk Y, Matisons R, Mionskowski M, Wojda T, Koprowski M, Jagodziński AM. Black locust (*Robinia Pseudoacacia* L.) range contraction and expansion in Europe under changing climate. Glob Chang Biol. 2021;27:1587–600. https://doi.org/10.1111/gcb.15486.
72. Bombi P, D'Andrea E, Rezaie N, Cammarano M, Matteucci G. Which climate change path are we following? Bad news from Scots pine. PLoS ONE. 2017;12:e0189468. https://doi.org/10.1371/journal.pone.0189468.
73. Dyderski M, Paź S, Frelich LE, Jagodziński AM. How much does climate change threaten European forest tree species distributions? Glob Chang Biol. 2018;24:1150–63. https://doi.org/10.1111/gcb.13925.
74. Skov F, Svenning JC. Potential impact of Climatic change on the distribution of forest herbs in Europe. Ecography. 2004;27:366–80. https://doi.org/10.1111/j.0906-7590.2004.03823.x.
75. Dong SL. The study on the characteristic of the seed dormancy and germination of parasitic drug plant——*Cynomorium Songaricum*. Gansu: Gansu agriculture university; 2011.
76. Warren DG, Richard EG, Michael T, ENMTools. A toolbox for comparative studies of environmental niche models. Ecography. 2010;33:607–11. https://doi.org/10.1111/j.1600-0587.2009.06142.x.
77. Chapin CT, Bridgham SD, Pastor J. pH and nutrient effects on above-ground net primary production in a Minnesota, USA bog and Fen. Wetlands. 2004;24(1):186–201. https://doi.org/10.1672/0277-5212(2004)024.
78. Hájek T. Physiological ecology of peatland bryophytes. In: Hanson DT, Rice SK, editors, Photosynthesis in bryophytes and early land plants. Springer; 2014. pp. 233–252. https://doi.org/10.1007/978-94-007-6988-5_13
79. Oke TA, Hager HA. Assessing environmental attributes and effects of climate change on sphagnum peatland distributions in North America using single- and multi-species models. PLoS ONE. 2017;12(4):e175978. https://doi.org/10.1371/journal.pone.017597825.
80. Popov SY. The Climatic patterning of sphagnum sect. Sphagnum species distribution in the East European plain. Arctoa. 2016;25(1):332–52. https://doi.org/10.15298/arctoa.25.26.
81. Popov SY. Distribution patterns of sphagnum sect. Acutifolia species in the Eastern European plain and Eastern Fennoscandia. Arctoa. 2018;27(1):34–48. https://doi.org/10.15298/arctoa.27.04.
82. Fick SE, Hijmans RJ. WorldClim 2: new 1-km Spatial resolution climate surfaces for global land areas. Int J Climatol. 2017;37:4302–15. https://doi.org/10.1002/joc.5086.
83. Puchałka R, Klisz M, Koniakin S, Czortek P, Dylewski Ł, Paź -Dyderska S, Vitkova M, Sadlo J, Rasomavicius V, Carni A, De Sanctis M, Dyderski M. Citizen science helps predictions of climate change impact on floweringphenology: a study on anemone Nemorosa. Agric Meteorol. 2022;325:109133. https://doi.org/10.1016/j.agrformet.2022.109133.
84. Thuiller W, Lavorel S, Araujo MB, Sykes MT, Prentice IC, Araújo MB. Climate change threats to plant diversity in Europe. Proc Natl Acad Sci. 2005;102:8245–50. https://doi.org/10.1073/pnas.0409902102.
85. Booth TH, Nix HA, Busby JR, Hutchinson MF. BIOCLIM: the first species distribution modelling package, its early applications and relevance to most current maxent studies. Divers Distrib. 2014;20:1–9. https://doi.org/10.1111/ddi.12144.
86. O'Donnell MS, Ignizio DA. Bioclimatic predictors for supporting ecological applications in the conterminous united States. In: U S Geol Surv Data Ser. 2012;691:10.
87. Riahi K, van Vuuren DP, Kriegler E, Edmonds J, O'Neill BC, Fujimori S, Bauer N, Calvin K, Dellink R, Fricko O, Lutz W, Popp A, Cuaresma JC, KC S, Leimbach M, Jiang L, Kram T, Rao S, Emmerling J, Ebi K, Hasegawa T, Havlik P, Humpenőder F, Da Silva LA, Smith S, Stehfest E, Bosetti V, Eom J, Gernaat D, Masui T, Rogelj J, Strefler J, Drouet L, Krey V, Luderer G, Harmsen M, Takahashi K, Baumstark L, Doelman JC, Kainuma M, Klimont Z, Marangoni G, Lotze-Campen H, Obersteiner M, Tabeau A, Tavoni M. The shared socioeconomic pathways and their energy, land use, and greenhouse gas emissions implications: an overview. Glob Environ Chang. 2017;42:153–68. https://doi.org/10.1016/j.gloenvcha.2016.05.009.
88. Araújo MB, New M. Ensemble forecasting of species distributions. Trends Ecol Evol. 2007;22(1):42–7. https://doi.org/10.1016/j.tree.2006.09.010.
89. Marmion M, Hjort J, Thuiller W, Luoto M. Statistical consensus methods for improving predictive geomorphology maps. Comput Geosci. 2009;35(3):615–25. https://doi.org/10.1016/j.cageo.2008.02.024.
90. Sillero N. What does ecological modelling model? A proposed classification of ecological niche models based on their underlying methods. Ecol Model. 2011;222(8):1343–6.
91. Thuiller W, Georges D, Engler R, Breiner F. biomod2: ensemble platform for species distribution modeling. R Package Version. 2021;351 3:r539.
92. Thuiller W, Georges D, Gueguen M, Engler R, Breiner F. Package 'biomod2': Version 3.5.1. 2021.
93. Xian XQ, Zhao HX, Wang R, Huang HK, Chen BX, Zhang GF, Liu WX, Wan FH. Climate change has increased the global threats posed by three ragweeds (Ambrosia L.) in the anthropocene. Sci Total Environ. 2023;859:160252. https://doi.org/10.1016/j.scitotenv.2022.160252.
94. Cohen J. A coefficient of agreement of nominal scales. Educ Psychol Meas. 1960;20:37–46.
95. Fielding A, Bell J. A review of methods for the assessment of prediction errors in conservation presence/absence models. Environ Conserv. 1997;24:38–49. https://doi.org/10.1017/S0376892997000088.
96. Peterson AT, Papeş M, Soberón J. Rethinking receiver operating characteristic analysis applications in ecological niche modeling. Ecol Model. 2008;213(1):63–72. https://doi.org/10.1016/j.ecolmodel.2007.11.008.
97. Allouche O, Tsoar A, Kadmon R. Assessing the accuracy of species distribution models: prevalence, kappa and the true skill statistic (TSS). J Appl Ecol. 2006;43(6):1223–32. https://doi.org/10.1111/j.1365-2664.2006.01214.x.
98. Schoener TW. The Anolis lizards of bimini: resource partitioning in a complex fauna. Ecology. 1968;49:704–26. https://doi.org/10.2307/1935534.
99. Warren DL, Glor RE, Turelli M. Environmental niche equivalency versus conservatism: quantitative approaches to niche evolution. Evolution. 2008;62:2868–83. https://doi.org/10.1111/j.1558-5646.2008.00482.x.


## Publisher's note

Springer Nature remains neutral with regard to jurisdictional claims in published maps and institutional affiliations.